China Ocean Engineering, Vol. 21, No. 3, pp. 429 - 437
©2007 China Ocean Press, ISSN 0890-5487

Variation of Added Mass and Its Application to the Calculation of Amplitude Response for A Circular Cylinder *

WANG Yi (王 艺), CHEN Wei-min (陈伟民)[1]
and LIN Mian (林 缅)
Institute of Mechanics, Chinese Academy of Sciences, Beijing 100080, *China*

(Received 3 August 2006; accepted 24 April 2007)

ABSTRACT

In the present study, analyzed are the variation of added mass for a circular cylinder in the lock-in (synchronization) range of vortex-induced vibration (VIV) and the relationship between added mass and natural frequency. A theoretical minimum value of the added mass coefficient for a circular cylinder at lock-in is given. Developed are semi-empirical formulas for the added mass of a circular cylinder at lock-in as a function of flow speed and mass ratio. A comparison between experiments and numerical simulations shows that the semi-empirical formulas describing the variation of the added mass for a circular cylinder at lock-in are better than the ideal added mass. In addition, computation models such as the wake oscillator model using the present formulas can predict the amplitude response of a circular cylinder at lock-in more accurately than those using the ideal added mass.

Key words: *vortex-induced vibration; added mass; lock-in; mass ratio; natural frequency*

1. Introduction

More and more deepwater platforms such as TLP, SPAR and FPSO are used in offshore gas and oil exploitation and production. When the depth of sea and the length of structure increase, the flexibility of the structure also increases. On the other hand, because ocean current and wave action are getting greater, interaction between fluid and structure becomes stronger. In particular, vortex-induced vibration (VIV) of risers and tension legs, especially in the lock-in (synchronization) range, has become a very challenging problem.

Up to now, some important results on VIV of a circular cylinder at lock-in have been obtained. Based on experimental results, Govardhan and Williamson (2000) gave the relationship between frequency ratio f^* ($f^* = f_{osc}/f_{n0}$) and reduced velocity U^* ($U/f_{n0}D$) for a circular cylinder at lock-in, where f_{osc} represents the oscillatory frequency of the circular cylinder, $f_{n0} = \frac{1}{2\pi}\sqrt{K/(m+m_D)}$ is the natural frequency of the circular cylinder in still water, U is the flow velocity, D is the diameter of the cylinder, K is the linear spring constant, m is the mass of the circular cylinder, and m_D is the displaced mass of fluid by the immersed body. Their results are shown in Fig. 1 and Fig. 2.

From Fig. 1 the following conclusions can be drawn: 1) The lock-in range can be divided into

* This work is financially supported by Projects 863 (2006AA09Z301), NSF (10532070) and KJCX2-YW-L02.
1 Corresponding author. E-mail: wmchen@imech.ac.cn

two parts: in the first part, frequency ratio f^* changes linearly with the reduced velocity U^*; in the second part, i.e. the lower branch, f^* does not change with U^* and keeps constant. 2) The reduced velocity range of the lock-in stage depends on mass ratio m^*, where $m^* = m/m_D$. 3) When $m^* \geq 10.0$, a cylinder almost directly turns into the second part as soon as it enters the lock-in range and $f^* \approx 1.0$.

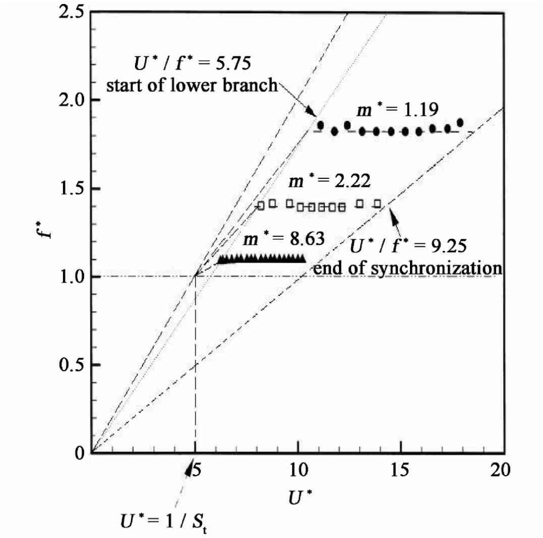

Fig. 1. The relationship among f^*, u^*, and m^* in the lock-in range when $(m^*\zeta)$ is very low. m^* is mass ratio. ζ is damping ratio. St is the Strouhal number. Horizontal lines represent the lower branch. (Govardhan and Williamson, 2000).

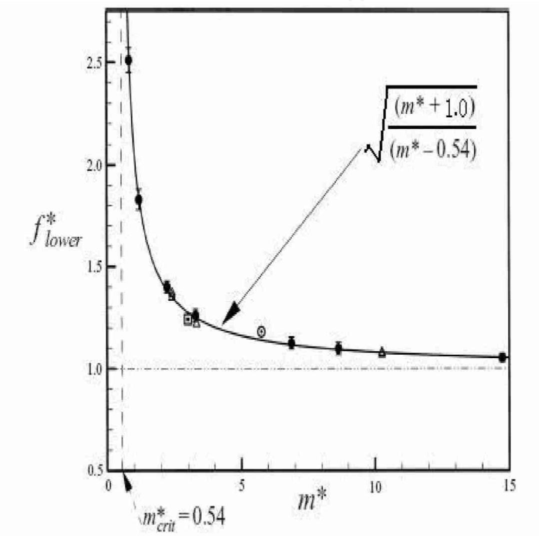

Fig. 2. Frequency versus mass ratio of a circular cylinder undergoing VIV at the lower branch. ● Govardhan (2000) △ Khalak (1999) □ Hover (1998) ⊙ Anand (1985) (Govardhan and Williamson, 2000).

Govardhan and Williamson (2000) also gave an empirical formula on the relationship between frequency ratio f^* and mass ratio m^* for a circular cylinder at the lower branch as shown in Fig. 2:

$$f^*_{\text{lower}} = \sqrt{\frac{m^* + 1.0}{m^* - 0.54}} \tag{1}$$

where $f^*_{\text{lower}} = f_{\text{lower}} / f_{n0}$, f_{lower} denoting the frequency of a circular cylinder at the lower branch of the lock-in range.

On the other hand, many computation models for cylinder's vortex-induced vibration such as the wake oscillator model, correlation model, statistic model and polynomial Galerkin model have also been developed to calculate the amplitude response of VIV.

In these semi-empirical models, added mass is an important quantity and the ideal added mass, i.e. the added mass for an accelerating body moving in an infinite, inviscid and incompressible fluid, is often adopted. For example, the ideal added mass coefficient is 0.5 for a sphere and 1.0 for a circular cylinder.

However, added mass in general is variable and not equal to the ideal added mass due to viscous effect. It is constant and equal to the ideal added mass only at the instant that the body started from rest in a fluid. Sarpkaya (2004a) pointed this out and did experiments (Sarpkaya, 1978, 2004b) to observe the fluid dynamic force (inertia component and drag component) on the body undergoing VIV. By definition, inertia component relates to added mass in the whole lock-in range of VIV. Vikestad's experiment (Vikestad *et al.*, 2000) showed that the added mass coefficient C_a ($C_a = m_a / m_D$, m_a being the added mass) for a circular cylinder varies from 4.5 to nearly -0.8 when the reduced velocity changes from 3.0 to 13.0. Thus experiments demonstrate very clearly that the added mass of a circular cylinder undergoing VIV can not be simply equal to the ideal added mass. The same conclusion is also drawn from numerical simulation (Willden and Graham, 2001). So the outstanding problem is how to show the variation of added mass for a circular cylinder at lock-in.

In this paper semi-empirical formulas for the added mass coefficient of a circular cylinder at lock-in will be given and applied to the calculation of the amplitude response of VIV with the wake oscillator model.

2. Theoretical Analysis

A spring-mass-damping model shown in Fig. 3 is adopted to study the added mass of a circular cylinder at lock-in. Two assumptions are given: 1. Stiffness of spring is constant; 2. Damping is very small.

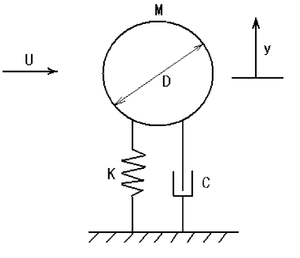

Fig. 3. spring-mass-damping model.

The governing equation of a circular cylinder subjected to VIV is:

$$m \frac{\mathrm{d}^2 y}{\mathrm{d} t^2} + 2\zeta m (2\pi f_0) \frac{\mathrm{d} y}{\mathrm{d} t} + m (2\pi f_0)^2 y = F_v(t), \tag{2}$$

where, m is the mass of the circular cylinder with unit length; f_0 is the natural frequency of the circular cylinder in vacuum and $f_0 = \frac{1}{2\pi}\sqrt{K/m}$; y is the displacement of the circular cylinder; ζ is the damping ratio, i.e. the ratio of structural damping to critical damping in water; $F_v(t)$ is the cross-flow component of the total hydrodynamic force.

At lock-in, a good approximation to the displacement of cylinder and the lift force of fluid (Sarpkaya, 1979) is

$$y(t) = A\sin(2\pi f_{osc} t), \quad F_v(t) = F_L \sin(2\pi f_{osc} t + \phi). \tag{3}$$

$F_v(t)$ can be rewritten as:

$$F_v(t) = F_L\cos\phi\sin(2\pi f_{osc}t) + F_L\sin\phi\cos(2\pi f_{osc}t). \tag{4}$$

Substituting Eq. (4) into Eq. (2), the following equation is obtained:

$$m\frac{d^2y}{dt^2} + 2\zeta m(2\pi f_0)\frac{dy}{dt} + m(2\pi f_0)^2 y = F_L\cos\phi\sin(2\pi f_{osc}t) + F_L\sin\phi\cos(2\pi f_{osc}t). \tag{5}$$

From Eq. (3) one obtains:

$$\frac{d^2y}{dt^2} = -A(2\pi f_{osc})^2\sin(2\pi f_{osc}t), \quad \frac{dy}{dt} = A(2\pi f_{osc})\cos(2\pi f_{osc}t). \tag{6}$$

Substituting Eq. (6) into Eq. (5) yields:

$$\left[m + \frac{F_L\cos\phi}{A(2\pi f_{osc})^2}\right]\frac{d^2y}{dt^2} + \left[2\zeta m(2\pi f_0) - \frac{F_L\sin\phi}{A(2\pi f_{osc})}\right]\frac{dy}{dt} + m(2\pi f_0)^2 y = 0. \tag{7}$$

According to the definition of added mass, the expression of added mass is

$$m_a = \frac{F_L\cos\phi}{A(2\pi f_{osc})^2}. \tag{8}$$

If damping is negligibly small, the following equation can be obtained from Eq. (7)

$$(m + m_a)\frac{d^2y}{dt^2} + m(2\pi f_0)^2 y = 0. \tag{9}$$

Eq. (9) is an equation of a single degree-of-freedom system describing harmonic oscillation with natural frequency

$$f_n = \frac{f_0}{\sqrt{1 + m_a/m}} \quad \text{or} \quad m_a = m(f_0^2/f_n^2 - 1). \tag{10}$$

Eq. (10) shows that the true nature frequency f_n of a cylinder at lock-in is controlled by the fluid via its added mass. Experiment (Vikestad *et al*., 2000) and numerical simulation (Willden and Graham, 2001) show that the oscillation frequency is nearly equal to the true natural frequency of a circular cylinder at lock-in.

Because f_0^2/f_n^2 is always positive at lock-in, the following equation is obtained from Eq. (10):

$$m_a > (-m) \tag{11}$$

Eq. (11) shows that the added mass can not be smaller than $-m$ in the lock-in range of VIV.

Eq. (1) requires $m^* > 0.54$, i.e. $-m < -0.54m_D$, and $m_a \geq -0.54m_D$ can be obtained from Eq. (11), therefore the theoretical minimum value of added mass coefficient for a circular cylinder at lock-in is $C_{a\min} = -0.54$.

3. Semi-Empirical Formulas for Added Mass

At lock-in frequency ratio can be written as:

$$f^* = \frac{f_{osc}}{f_{n0}} = \frac{f_n}{f_{n0}} = \sqrt{\frac{m + m_D}{m + m_a}}. \tag{12}$$

The estimation formulas of added mass coefficient for a circular cylinder at lock-in will be given for two separate cases, $m^* < 10.0$ and $m^* \geq 10.0$.

3.1 Mass Ratio $m^* < 10.0$

The intersection point of two parts in the lock-in range of VIV is determined by $\frac{U^*}{f^*} = 5.75$ and $f^*_{lower} = \sqrt{\frac{m^* + 1.0}{m^* - 0.54}}$.

In the first part, $\frac{f^* - 1.0}{U^* - 5.0} = \frac{f^*_{lower} - 1.0}{5.75 f^*_{lower} - 5.0}$, where $f^* = \sqrt{\frac{m + m_D}{m + m_a}}$. Thus, $f^* = \frac{f^*_{lower} - 1.0}{5.75 f^*_{lower} - 5.0}(U^* - 5.0) + 1.0$, i.e. $\sqrt{\frac{m + m_D}{m + m_a}} = \frac{f^*_{lower} - 1.0}{5.75 f^*_{lower} - 5.0}(U^* - 5.0) + 1.0$. Therefore, the added mass coefficient can be obtained:

$$C_a = \frac{m^* + 1}{G^2} - m^*, \text{ when } 5.75 f^*_{lower} > U^* > 5.0 \tag{13}$$

where, $G = \frac{f^*_{lower} - 1.0}{5.75 f^*_{lower} - 5.0}(U^* - 5.0) + 1.0$.

In the second part, because $f^* = f^*_{lower}$, i.e. $\sqrt{\frac{m + m_D}{m + m_a}} = \sqrt{\frac{m^* + 1.0}{m^* - 0.54}}$, the added mass coefficient is

$$C_a = -0.54, \quad \text{when} \quad 9.25 f^*_{lower} > U^* \geq 5.75 f^*_{lower}. \tag{14}$$

3.2 Mass Ratio $m^* \geq 10.0$

Under this condition, $f^* = f^*_{lower} \approx 1.0$, i.e. $\sqrt{\frac{m + m_D}{m + m_a}} = \sqrt{\frac{m^* + 1.0}{m^* - 0.54}}$, therefore, $m_a = -0.54 m_D$ can be obtained, i.e.

$$C_a = -0.54, \quad \text{when} \quad 9.25 f^*_{lower} > U^* > 5.0. \tag{15}$$

Eqs. (13) ～ (15) are the semi-empirical formulas for the added mass of a circular cylinder at lock-in.

3.3 Preconditions

Figs. 1 and 2 are obtained under the condition $m^* \zeta \leq 0.02$, which is obtained from the experimental data (Khalak and Williamson, 1997a, 1999). In Fig. 1, the reduced velocity at lock-in starts from $U^* = 1/St = 5.0$, where St is the Strouhal number and $St = 0.2$ is satisfied only when $100000 > Re > 300$ (Fernando and Hassan, 2005). In addition, Eq. (1) requires $m^* \geq 0.54$.

Therefore, Semi-empirical formulas on added mass for a circular cylinder at lock-in, i.e. Eqs. (13) ～ (15), should be used under the following conditions: $100000 > Re > 300$, $m^* \geq 0.54$ and $m^* \zeta \leq 0.02$.

4. Comparison Between Experiments and Numerical Simulations

For the verification of the semi-empirical formulas, Eqs. (13) ～ (15) will be compared with numerical simulations and experiments respectively.

Fig. 4 presents the comparison between the semi-empirical formulas and numerical simulation (Willden and Graham, 2001) using a quasi-three-dimensional numerical method. Eqs. (13) ~ (15) agree with the numerical simulation well, especially at low reduced velocity.

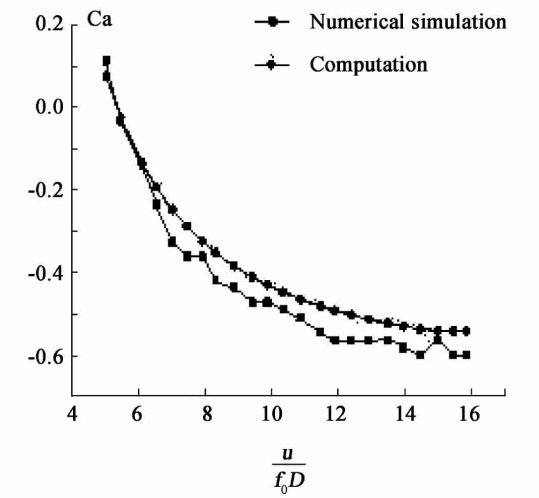

Fig. 4. Comparison with numerical simulation ($m^* = 0.6366$).

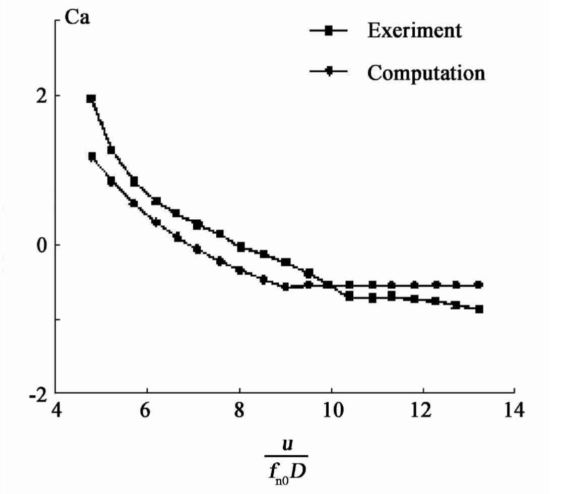

Fig. 5. Comparison with experimental results ($m^* = 1.6552$).

Fig. 5 shows that the results obtained from Eqs. (13)~(15) have the same tendency versus the reduced velocity as the experimental results (Vikestad *et al*., 2000).

For the case of low $m^* \zeta$, Fig. 2 (Govardhan and Williamson, 2000) shows that added mass coefficient keeps $C_a = -0.54 \pm 0.02$ at the lower branch of the lock-in range.

In the case of high mass ratio $m^* > 10.0$, Sarpkaya (1978, 2004b) made the VIV experiments of circular cylinders. These experiments showed that a circular cylinder with mass ratio $m^* > 10.0$ can be regarded to be in the second part as soon as it enters the lock-in range of VIV and added mass coefficient is $C_a \approx -0.50$, which is close to -0.54, the value presented by Eq. (15).

5. Application to the Wake Oscillator Model

5.1 The Modified Wake Oscillator Model

The wake oscillator model presented by Iwan (1974, 1975, 1981) is widely used to calculate the amplitude response of cylindrical structure (Lyons and Patel, 1986; Chen and Wang, 2004). Because of the variation of added mass at lock-in, this analytical model should be modified by using the added mass presented by Eqs. (13)~(15). The approaches of the modified wake oscillator model are suggested as follows:

(1) Calculate the natural frequency f_n and the mode shape of cylindrical structure $\xi_n(x)$ with the structural mass including the added mass m_a given by Eqs. (13)~(15).

(2) According to the flow speed distribution, the lock-in range along the cylindrical structure can

be decided. Function $s(x)$ is defined as:

$$s(x) = \begin{cases} 1, \text{when } 5.0 \le U^* \le 9.25 f^*_{\text{lower}}, \text{ for those parts at lock-in} \\ 0, \text{when } U^* < 5.0 \text{ or } U^* > 9.25 f^*_{\text{lower}}, \text{ for those parts out of lock-in} \end{cases}$$

(3) The effective mass $v_n = \int_0^L m(x)\xi_n^2(x)\,\mathrm{d}x \Big/ \int_0^L s(x)\xi_n^2(x)\,\mathrm{d}x$ and the mode shape factor $I_n = \int_0^L m(x)\xi_n^4(x)\,\mathrm{d}x \Big/ \int_0^L m(x)\xi_n^2(x)\,\mathrm{d}x$ are calculated, where $m(x)$ is the mass per unit length of the circular cylinder including the added mass obtained with Eqs. (13)～(15).

(4) Calculate the damping ratio ζ_n^S and the amplification factor F_n by iteration as follows:

Step 1. Assume the initial value of damping ratio ζ_n^I.

Step 2. Calculate the amplification factor $F_n = 1/[1 + 9.6(\mu_r^n \zeta_n^I)^{1.8}]$, where $\mu_r^n = \dfrac{v_n}{\pi\rho D^2/4}$.

Step 3. Calculate the damping ratio $\zeta_n^S = \zeta_n^I + F_n \Phi_n$, where

$$\Phi_n = (2D/3\pi)\frac{\int_0^L \rho C_D(x) D(x)[1 - s(x)]\,|\xi_n(x)|^3\,\mathrm{d}x}{\left[\int_0^L m(x)\xi_n^4(x)\,\mathrm{d}x\right]^{1/2}\left[\int_0^L m(x)\xi_n^2(x)\,\mathrm{d}x\right]^{1/2}}.$$

Step 4. If the damping ratio ζ_n^S and the amplification factor F_n do not satisfy the demand of convergence, then $\zeta_n^I = \zeta_n^S$ and go to step 2. Else, stop iteration.

(5) Calculate the amplitude of the cylinder at lock-in $Y_n(x) = DF_n I_n^{-1/2}\xi_n(x)$.

(6) According to the range of reduced velocity, correct the amplitude.

5.2 The Amplitude Response at Lock-in

The added mass coefficient given by Eqs. (13)～(15) and the ideal added mass coefficient of a circular cylinder are both used to calculate the amplitude response at lock-in and compared with the experimental results given by Khalak and Williamson (1997b). The approaches presented in section 5.1 are used and the results are presented in Fig. 6. It shows that the modified wake oscillator model using the added mass obtained from Eqs. (13)～(15) is more accurate than that using the ideal added mass.

6. Conclusion

Variation of the added mass for a circular cylinder at lock-in can be described better with semi-empirical formulas, i.e. Eqs. (13)～(15), than with the ideal added mass. The semi-empirical formulas show that added mass coefficient C_a for a circular cylinder at lock-in is mainly related to mass ratio m^* and reduced velocity U^*, i.e. $C_a = f(m^*, U^*)$. Theoretical minimum value of the added mass coefficient for a circular cylinder at lock-in is $C_{a\min} = -0.54$. In addition, the wake oscillator model using Eqs. (13)～(15) can predict the amplitude response of a circular cylinder at lock-in more accurately than that using the ideal added mass.

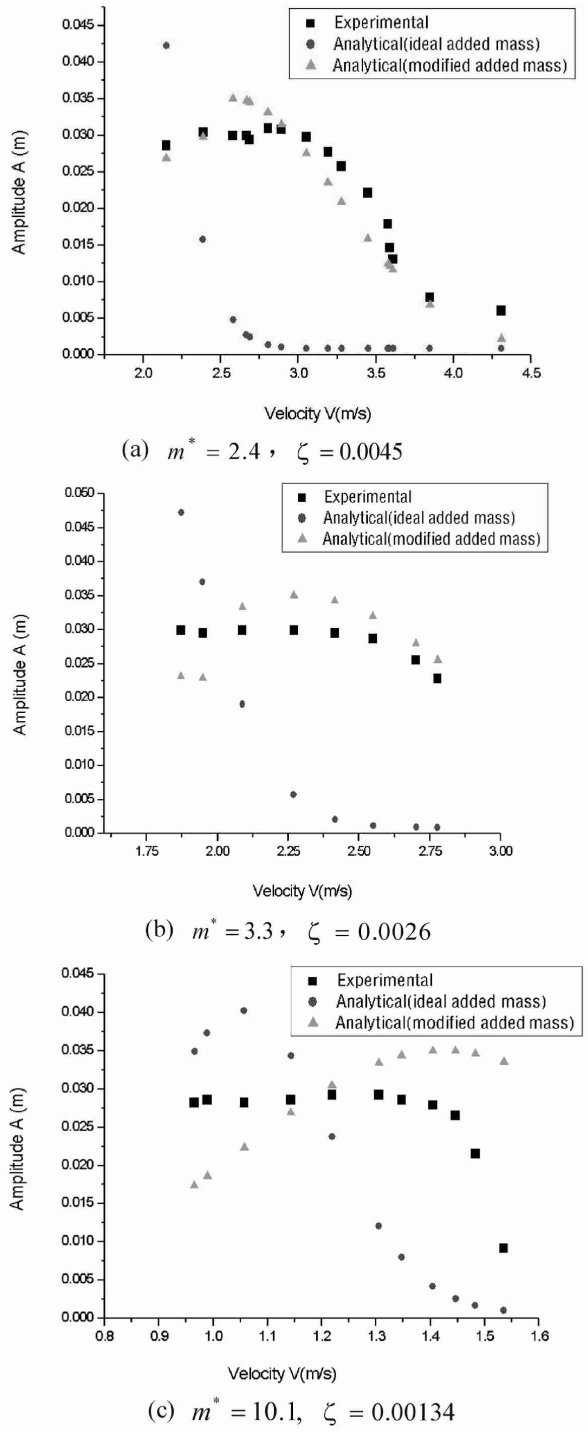

(a) $m^* = 2.4$, $\zeta = 0.0045$

(b) $m^* = 3.3$, $\zeta = 0.0026$

(c) $m^* = 10.1$, $\zeta = 0.00134$

Fig. 6. Comparison of amplitude responses at lock-in obtainde from calculation with those obtained from experiment.

References

Brika, D. and Laneville, A., 1993. Vortex-induced vibrations of a long flexible circular cylinder, *J. Fluid Mech.*, **250**, 481～506.

Chen Weimin and Wang Yi, 2004. The effect of tension and current distribution on vortex-induced vibration of tendon, *Shipbuilding of China*, **45** (z1): 226～232. (in chinese)

Fernando, L. P. and Hassan, A., 2005.. Vortex synchronization regions in shedding from an oscillating cylinder, *Physics of Fluids*, **17**(011703): 1～4.

Govardhan, R. and Williamson, C. H. K., 2000. Modes of vortex formation and frequency response of a freely vibrating cylinder, *J. Fluid Mech.*, **420**, 85～130.

Iwan, W. D. and Blevins, R. D., 1974. A model for the vortex-induced oscillation of structures, *Journal of Applied Mechanics*, ASME, **41**, 581～586.

Iwan, W. D., 1975. The vortex-induced oscillation of elastic structural elements, *Journal of Applied Mechanics*, ASME, **97**, 1378～1382.

Iwan, W. D., 1981. The vortex-induced oscillation of non-uniform structure analysis, *Journal of Sound and Vibration*, **79**(2): 291～301.

Khalak, A. and Williamson, C. H. K., 1997a. Investigation of relative effects of mass and damping in vortex-induced vibration of a circular cylinder, *Journal of Wind Engineering and Industrial Aerodynamics*, **69** - **71**, 341～350.

Khalak, A. and Williamson, C. H. K., 1997b. Fluid forces and dynamics of a hydroelastic structure with very low mass and damping, *Journal of Fluids and Structure*, **11**, 973～982.

Khalak, A. and Williamson, C. H. K., 1999. Motions, forces and mode transitions in vortex-induced vibrations at low mass-damping, *Journal of Fluids and Structure*, **13**, 813～851.

Lyons, G. J. and Patel, M. H., 1986. A prediction technique for vortex induced transverse response of marine risers and tethers, *Journal of Sound and Vibration*, **111**(3): 467～487.

Sarpkaya, T., 1978. Fluid forces on oscillating cylinders, *Journal of Waterway Port Coastal and Ocean Division*, ASCE, **104**(WW4): 275～290.

Sarpkaya, T., 1979. Vortex-induced oscillations, a selective review, *Journal of Applied Mechanics*, **46**, 241～258.

Sarpkaya, T., 2004a. A critical review of the intrinsic nature of vortex-induced vibrations, *Journal of Fluids and Structures*, **19**, 389～447.

Sarpkaya, T., 2004b. *Fluid forces on oscillating cylinders at various Reynolds numbers* (2.5×10^3, 7.5×10^3, 12.5×10^3, 15×10^3, 20×10^3, 45×10^3), Technical Report.

Vikestad, K., Vandiver, J. K. and Larsen, C. M., 2000. Added mass and oscillation frequency for a circular cylinder subjected to vortex-induced vibrations and external disturbance, *Journal of Fluids and Structures*, **14**, 1071～1088.

Willden, R. H. J. and Graham, J. M. R., 2001. Numerical prediction of VIV on long flexible circular cylinders, *Journal of Fluids and Structures*, **15**, 659～669.